Results in Chemistry 6 (2023) 101076

Contents lists available at ScienceDirect

Results in Chemistry

journal homepage: www.sciencedirect.com/journal/results-in-chemistry

Integration of DOTA as a bridging unit during solid-phase peptide synthesis

Lennard Wendlinger [a,b,c,*], Mara Parzinger [c], Margret Schottelius [a,b], Hans-Jürgen Wester [c]

[a] Translational Radiopharmaceutical Sciences, Centre Hospitalier Universitaire Vaudois, 1011, Switzerland
[b] AGORA, Pôle de recherche sur le cancer, 1011 Lausanne, Switzerland
[c] Pharmaceutical Radiochemistry, Technical University of Munich, 85748, Germany

ARTICLE INFO

Keywords:
Chelator
Bridging Unit
Radiopharmaceuticals
Solid-Phase Peptide Synthesis
Radiohybrid Tracers

ABSTRACT

A method for the introduction of bifunctionalized 1,4,7,10-tetraazacyclododecane-*N*,*N*',*N*'',*N*'''-tetraacetic acid (DOTA) into the bridging unit of peptide-based radiopharmaceuticals has been developed. The method is executed in the context of Fmoc-based solid-phase peptide synthesis (SPPS) using standard coupling reagents (HOAt, TBTU, DIPEA) and was optimized to maximize yields (>99% conversion) and suppress the formation of side products (<25%). The bifunctionalized DOTA chelator can be used to integrate radioactive or non-radioactive Ga^{3+}-isotopes. This facilitates novel and structurally simple PET tracer designs and the combination of other functional moieties, such as dyes, with Ga-DOTA-chelates in one hybrid tracer.

Introduction

Novel multimodal imaging approaches such as hybrid (fluorescence/radioactive) imaging and surgical guidance [1,2] or the implementation of the recently introduced radiohybrid (rh) concept [3] add a new level of complexity to the structural design of targeted probes with appropriate in vitro and in vivo characteristics.

The classical, linear peptide tracer design (chelator-pharmacophore or chelator-linker- pharmacophore) constitutes the structural basis of virtually all radiometal-labeled peptide tracers currently used in the clinic [4]. The integration of additional functionalities (fluorescent dye, pharmacokinetic modifiers, prosthetic groups for ^{18}F-labeling etc.) often requires the introduction of a trifunctional linker (e.g. an additional lysine residue). In many cases, such as in SiTATE [5], hybrid prostate-specific membrane antigen (PSMA)-ligands [6] or rh PSMA-analogs [3], this branching concept proved sufficient for generating tracers with appropriate in vitro and in vivo profiles. To simplify the design of bimodal (or hybrid) tracers and to accommodate even more functionalities, further branching can be envisioned [7]. However, such designs yield complex, high molecular weight compounds and entail challenges for protecting group strategies and synthetic accessibility.

In a pilot study of our group, the implementation of the rh concept (DOTA chelator and silicon fluoride acceptor (SiFA) moiety) in somatostatin receptor 2 (sst_2) targeted Tyr^3-octreotate (TATE, D-Phe-cyclo [L-Cys-L-Tyr-D-Trp-L-Lys-L-Thr-L-Cys]-L-Thr) ligands was attempted in analogy to the design of the recently approved rh PSMA ligand [^{18}F][Ga]rhPSMA-7.3 (POSLUMA), using one single branching unit [3]. Although synthetically successful, this approach led to sst_2-targeted tracers with diminished affinity, probably caused by the loss of the TATE adjacent [Ga]DOTA moiety, which is known to greatly enhance ligand affinity [8]. Furthermore, the compounds were highly lipophilic, necessitating the introduction of an additional pharmacokinetic modifier.

As shown in the literature, the stable chelation of Ga^{3+} only requires two of the four carboxylate pendant arms available in the DOTA chelator [9]. When coupled to the pharmacophore, one of the two redundant carboxylate arms is engaged in the amide bond to the peptide pharmacophore, but the other remains free. It was thus the objective of this study to exploit this free carboxylate functionality to use the DOTA chelator as a bridging unit in the context of the SPPS of sst_2-targeted rh ligands. This approach was expected to reduce the structural complexity of SiFA-based rh sst_2-ligands and to allow the introduction of additional pharmacokinetic modifiers to finetune in vitro and in vivo tracer characteristics.

Materials and methods

Synthesis of Fmoc-TATE(PG)-2-CT

The synthesis of resin-bound Fmoc-TATE(PG)-2-CT was carried out according to a procedure by *Niedermoser et al* [10]. Detailed protocols are provided in the supplemental information. Briefly, 2-CT resin is loaded with Fmoc–L–Thr(*t*Bu)–OH (resin occupancy: 0.5–0.7 mmol/g).

* Corresponding author at: Translational Radiopharmaceutical Sciences, Centre Hospitalier Universitaire Vaudois, 1011, Switzerland.
E-mail address: Lennard.wendlinger@chuv.ch (L. Wendlinger).

https://doi.org/10.1016/j.rechem.2023.101076
Received 3 July 2023; Accepted 21 August 2023
Available online 23 August 2023
2211-7156/© 2023 The Author(s). Published by Elsevier B.V. This is an open access article under the CC BY license (http://creativecommons.org/licenses/by/4.0/).

After Fmoc-deprotection using 20% piperidine in DMF, Fmoc-L-Cys (Acm)-OH was coupled, followed by Fmoc-L-Thr(*t*Bu)-OH, Fmoc-L-Lys (Boc)-OH, Fmoc-D-Trp(Boc)-OH, Fmoc-L-Tyr(*t*Bu)-OH, Fmoc-L-Cys (Acm)-OH and Fmoc-D-Phe-OH. Oxidative cyclization of the resulting peptide-chain with simultaneous deprotection of the Acm-protecting groups was carried out using Thallium(III) trifluoroacetate [11], yielding the resin-bound Fmoc-TATE(PG)-2-CT. After most reaction steps, test cleavages using 95% trifluoroacetic acid (TFA) were carried out to confirm quantitative coupling/cyclisation.

RP-HPLC (anal.; 10–90% MeCN/H_2O (0.1% TFA, *v/v)* in 15 min): t_R = 10.8 min; K' = 4.1.

ESI-MS (positive ion mode): *m/z* calculated for $C_{64}H_{74}N_{10}O_{14}S_2$: 1270.48, found: 1315.1 $[M + CO_2 + H]^+$.

Synthesis of two exemplary ligands

Synthesis of SSA1

Somatostatin analogue 1 (SSA1) was synthesized based on the above Fmoc-TATE(PG)-2-CT precursor. Upon Fmoc-deprotection, DOTA(*t*Bu)$_2$ was coupled to the resin-bound peptide (see GSP7 in the supplementary materials). Subsequently, Fmoc-D-Dap-O*t*Bu, Dimethylglycine hydrochloride and SiFA-Br were coupled using the respective optimized protocols (see supplementary material). The product was cleaved from the resin with simultaneous removal of all acid-labile groups using TFA, purified via preparative RP-HPLC, and lyophilized.

SSA1:

= *N*-SiFA*lin-N,N*-Me_2-Gly-D-Dap(*trans*-DOTA-TATE)-OH.

RP-HPLC (anal.; MeCN/H_2O (0.1% TFA, *v/v)* in 15 min): t_R = 12.6 min; K' = 5.0.

RP-HPLC (prep.): (35–47% MeCN/H_2O (0.1% TFA, *v/v)* in 20 min): t_R = 17.2 min; K' = 5.2.

ESI-MS (positive ion mode): *m/z* calculated for $C_{87}H_{127}FN_{17}O_{21}S_2Si^+$: 1856.86, found: 619.9 $[M + 3H]^{3+}$, 929.3 $[M + 2H]^{2+}$.

Synthesis of SSA2

SSA2 was synthesized based on the 2-CT-TATE(PG)-Fmoc precursor. Upon Fmoc-deprotection, DOTA(*t*Bu)$_2$ was coupled to the resin-bound peptide (see GSP7 in the supplementary materials). Subsequently, Fmoc-D-Lys-O*t*Bu, Dimethylglycine hydrochloride and SiFA-Br were coupled using the respective optimized protocols (see supplementary material). The product was cleaved from the resin with simultaneous removal of all acid-labile groups using TFA, purified via preparative RP-HPLC, and lyophilized.

SSA2:

N-SiFA*lin-N,N*-Me_2-Gly -D-Lys(*trans*-DOTA-TATE)-OH.

RP-HPLC (anal.; 10–60% MeCN/H_2O (0.1% TFA, *v/v)* in 15 min): t_R = 12.7 min; K' = 5.0.

RP-HPLC (prep; 33–50% MeCN/H_2O (0.1% TFA, *v/v)* in 20 min): t_R = 18.5 min; K' = 5.5.

ESI-MS (positive ion mode): *m/z* calculated for $C_{90}H_{133}FN_{17}O_{21}S_2Si^+$: 1898.91, found: 634.0 $[M + 3H]^{3+}$, 950.3 $[M + 2H]^{2+}$, 1899.8 $[M + H]^+$.

Complex formation with ^{nat}Ga

For the incorporation of ^{nat}Ga into the DOTA chelator, a 2 mM solution of SSA1 and SSA2 in dimethylsulfoxide (DMSO), respectively, is added to a solution of $Ga(NO_3)_3$ (20 mM in H_2O, 1.5 eq.) and diluted to 1 mM by the addition of DMSO. The respective mixtures were heated to 70 °C for 1 h, resulting in quantitative complex formation.

[^{nat}Ga]SSA1:

N-SiFA*lin-N,N*-Me_2-Gly-D-Dap(*trans*-[^{nat}Ga]DOTA-TATE)-OH.

RP-HPLC (anal; 10–60% MeCN/H_2O (0.1% TFA, *v/v)* in 15 min): t_R = 13.1 min; K' = 5.2.

ESI-MS (positive ion mode): *m/z* calculated for $C_{87}H_{125}FGaN_{17}O_{21}S_2Si^+$: 1923.77, found: 642.2 $[M + 3H]^{3+}$, 962.7 $[M + 2H]^{2+}$, 1283.5 $[2\ M + 3H]^{3+}$.

[^{nat}Ga]SSA2:

N-SiFA*lin-N,N*-Me_2-Gly-D-Lys(*trans*-[^{nat}Ga]DOTA-TATE)-OH.

RP-HPLC (anal.; 10–60% MeCN/H_2O (0.1% TFA, *v/v)* in 15 min): t_R = 13.2 min; K' = 5.3.

ESI-MS (positive ion mode): *m/z* calculated for $C_{90}H_{131}FGaN_{17}O_{21}S_2Si^+$: 1965.82, found: 656.2 $[M + 3H]^{3+}$, 983.8 $[M + 2H]^{2+}$, 1311.8 $[2\ M + 3H]^{3+}$.

Results and discussion

A scheme for the general reaction of DOTA(*t*Bu)$_2$ with the *N*-terminal amine of protected, resin-bound TATE (H_2N-TATE(PG)-2CT, H_2N-D-Phe-cyclo[L-Cys-L-Tyr(*t*Bu)-D-Trp(Boc)-L-Lys(Boc)-L-Thr(*t*Bu)-L-Cys]-L-Thr(*t*Bu)-2CT) is shown in Fig. 1.

Using resin-bound H_2N-TATE(PG)-2CT typically loaded with 0.72 ± 0.02 mmol H_2N-TATE(PG)-2CT per g, we initially used standard coupling conditions for direct *N*-terminal conjugation of DOTA(*t*Bu)$_2$. After 2 h, no product formation was observed by reversed-phase high performance liquid chromatography (RP-HPLC, λ = 214 nm) (Table 1, entry 1). Modifying the number of equivalents of DOTA(*t*Bu)$_2$ or of the coupling reagents also did not lead to any product formation after 2 h (entry 2–4). Upon continuing the reaction overnight, improved product formation was observed. However, this was accompanied by an unwanted side-product that seemed to stem from on-resin dimerization (entry 5). Formation of this dimer significantly lowers the synthetic yields of the desired product, prompting us to further optimize the reaction conditions such as to suppress the dimerization.

Since the side-product is the result of the activation of both free carboxylates of DOTA(*t*Bu)$_2$, we attempted to suppress this by introducing increased amounts of DOTA(*t*Bu)$_2$ (entry 6). Statistically, this was expected to suppress the formation of the di-activated species and to favor the formation of the product. Indeed, a lower degree of dimerization was observed. In agreement with the underlying hypothesis, the reaction in the presence of an excess of coupling reagents (entry 7) led to increased dimer formation (as well as higher overall conversion rates).

To increase the yield of the coupling reaction, different coupling reagents were investigated (entry 8–10), none of which provided improved results. Further investigations involving higher equivalents of DOTA(*t*Bu)$_2$ (entry 11), longer preactivation times (entry 12), consecutive addition of the active ester solution (entry 13), strict control of the pH at 8–9 (entry 14) or coupling to uncyclized H_2N-TATE(PG)-2CT followed by cyclization using $Tl(CF_3CO_2)_3$ [11] (not shown) also had no positive impact on the reaction.

Further batches of Fmoc-TATE(PG)-2CT were thus prepared with lower resin-loading (0.51 ± 0.01 mmol/g; n = 4). This was found to disfavor the dimerization and consistently provided > 75% of the desired monomer using the reaction conditions described in entry 15. The small remaining fraction of dimeric side-product (ca. 10–25%) does not interfere with the subsequent steps of SPPS and is easily removed from the product by preparative RP-HPLC at a later stage.

Upon successful coupling of DOTA(*t*Bu)$_2$ to TATE(PG)-2CT, the remaining free carboxylate of the peptide-resin bound DOTA(*t*Bu)$_2$ was then converted to an active ester by the addition of a solution of HOAt (1.5 eq.), TBTU (1.5 eq.) and DIPEA (4.5 eq.) for 10 mins. A solution of Fmoc-D-Lys-O*t*Bu (1.5 eq.) was added to extend the linker and convert the *N*–terminus to a Fmoc-protected primary amine, which is suitable for standard solid-phase peptide synthesis. The reaction scheme is given in Fig. 2. This step was completed quantitatively based on RP-HPLC.

Based on this method, we were able to successfully synthesize a series of novel rh sst_2 ligands containing *N*-terminal pharmacokinetic modifiers as well as a SiFA*lin*-moiety which allows for radiolabeling with ^{18}F. The capacity of DOTA to complex Ga^{3+} remains unaffected by its integration into the linker, as was confirmed by the quantitative formation of the ^{nat}Ga complexes of the respective compounds.

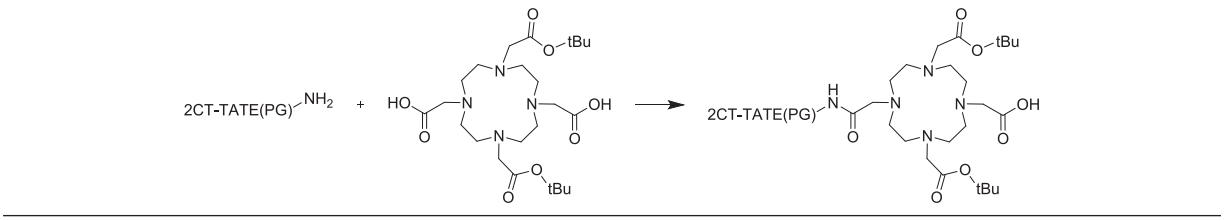

Fig. 1. Synthetic scheme for the coupling of DOTA(tBu)$_2$ to resin-bound TATE with protected sidechain functionalities.

Table 1
Tested reaction conditions for the coupling of DOTA(tBu)$_2$ with approximate yields as determined by analytical RP-HPLC ($\lambda = 214$ nm). Unknown side products are not quantified.

	Conditions	Resin load [mmol/g]	Coupling reagents [eq.]	DOTA(tBu)$_2$ [eq.]	Time	Starting-material	Product	Dimer
1	HOAt/TBTU	0.72 ± 0.02	1.5	1.5	2 h	>99%	0%	0%
2	HOAt/TBTU	0.72 ± 0.02	1.5	2.0	2 h	>99%	0%	0%
3	HOAt/TBTU	0.72 ± 0.02	1.5	3.0	2 h	>99%	0%	0%
4	HOAt/TBTU	0.72 ± 0.02	1.1	1.5	2 h	>99%	0%	0%
5	HOAt/TBTU	0.72 ± 0.02	1.5	1.5	15 h	40%	42%	18%
6	HOAt/TBTU	0.72 ± 0.02	1.5	3.0	15 h	49%	41%	10%
7	HOAt/TBTU	0.72 ± 0.02	3.0	1.5	15 h	12%	27%	44%
8	HOAt/HATU	0.72 ± 0.02	1.5	1.5	15 h	43%	41%	16%
9	EDCI/NHS	0.72 ± 0.02	2.0	2.0	15 h	3%	36%	9%
10	DIC/Oxyma	0.72 ± 0.02	4.0/2.0	5.0	15 h	>99%	0%	0%
11	HOAt/TBTU	0.72 ± 0.02	1.5	5.0	15 h	90%	6%	0%
12	HOAt/TBTU(Long activation)	0.72 ± 0.02	1.5	5.0	15 h	94%	4%	2%
13	HOAt/TBTU (Consecutive addition)	0.72 ± 0.02	1.5	5.0	15 h	>99%	0%	0%
14	HOAt/TBTU(pH = 8–9)	0.72 ± 0.02	1.5	5.0	48 h	96%	4%	0%
15	HOAt/TBTU	0.51 ± 0.01	1.5	3.0	15 h	<1%	>75%	<25%

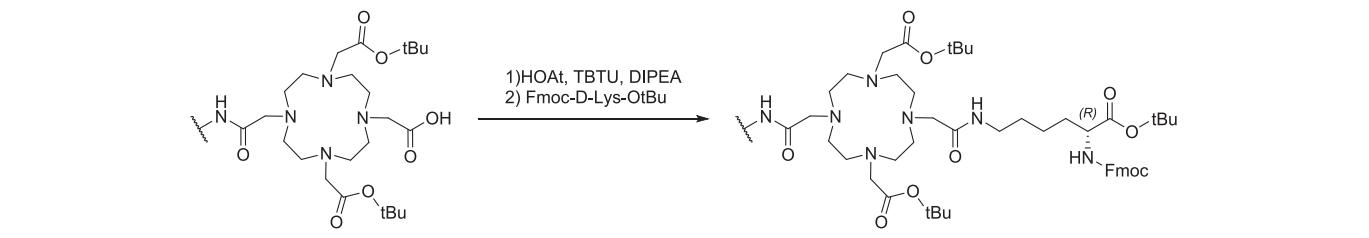

Fig. 2. Scheme for the coupling of Fmoc-D-Lys-OtBu to the resin-bound DOTA bridging unit.

Conclusion

In summary, a synthetic strategy for the incorporation of DOTA as a bridging unit during SPPS was successfully implemented and optimized, leading to high yields of the desired product and efficient suppression of side product formation. This synthetic strategy allows access to a series of novel sst$_2$ targeted rh tracers containing additional functionalities. Generally, the introduction of the DOTA-chelator as a bridging unit may serve as a valuable synthetic concept for a variety of multifunctional ^{68}Ga-labeled imaging probes with compact molecular designs.

CRediT authorship contribution statement

Lennard Wendlinger: Methodology, Formal analysis, Investigation, Writing – original draft. **Mara Parzinger:** Conceptualization, Methodology, Investigation, Supervision, Writing – review & editing. **Margret Schottelius:** Writing - review & editing. **Hans-Jürgen Wester:** Conceptualization, Project administration, Funding acquisition, Writing – review & editing.

Declaration of Competing Interest

The authors declare the following financial interests/personal relationships which may be considered as potential competing interests: [The authors (LW, MP and HJW) are listed as inventors on the patent EP2022/071964 “Ligand compounds comprising a chelating group as a bridging unit”.].

References

[1] N.S. van den Berg, O.R. Brouwer, W.M.C. Klop, B. Karakullukcu, C.L. Zuur, I. B. Tan, A.J.M. Balm, M.W.M. van den Brekel, R.A. Valdés Olmos, F.W.B. van Leeuwen, Concomitant radio-and fluorescence-guided sentinel lymph node biopsy in squamous cell carcinoma of the oral cavity using ICG-99m Tc-nanocolloid, Eur. J. Nucl. Med. Mol. Imaging 39 (7) (2012) 1128–1136.
[2] M. Schottelius, et al., Synthesis and preclinical characterization of the PSMA-targeted hybrid tracer PSMA-I&F for nuclear and fluorescence imaging of prostate cancer, J. Nucl. Med. 60 (1) (2019) 71–78.
[3] A. Wurzer, D. Di Carlo, A. Schmidt, R. Beck, M. Eiber, M. Schwaiger, H.-J. Wester, Radiohybrid ligands: a novel tracer concept exemplified by 18F-or 68Ga-labeled rhPSMA inhibitors, J. Nucl. Med. 61 (5) (2020) 735–742.
[4] A.W. Hensbergen, T. Buckle, D.M. van Willigen, M. Schottelius, M.M. Welling, F. A. van der Wijk, T. Maurer, H.G. van der Poel, G. van der Pluijm, W.M. van Weerden, H.-J. Wester, F.W.B. van Leeuwen, Hybrid tracers based on cyanine backbones targeting prostate-specific membrane antigen: tuning pharmacokinetic properties and exploring dye–protein interaction, J. Nucl. Med. 61 (2) (2020) 234–241.
[5] S. Litau, S. Niedermoser, N. Vogler, M. Roscher, R. Schirrmacher, G. Fricker, B. Wängler, C. Wängler, Next generation of SiFA lin-based TATE derivatives for PET imaging of SSTR-positive tumors: influence of molecular design on in vitro

SSTR binding and in vivo pharmacokinetics, Bioconjug. Chem. 26 (12) (2015) 2350–2359.
[6] A.W. Hensbergen, et al., Image-guided surgery: are we getting the most out of small-molecule prostate-specific-membrane-antigen-targeted tracers? Bioconjug. Chem. 31 (2) (2019) 375–395.
[7] Y.H.W. Derks, S.A.M. van Lith, H.I.V. Amatdjais-Groenen, L.W.M. Wouters, A. Kip, G.M. Franssen, P. Laverman, D.W.P.M. Löwik, S. Heskamp, M. Rijpkema, Theranostic PSMA ligands with optimized backbones for intraoperative multimodal imaging and photodynamic therapy of prostate cancer, Eur. J. Nucl. Med. Mol. Imaging 49 (7) (2022) 2425–2435.
[8] J.C. Reubi, J.-C. Schär, B. Waser, S. Wenger, A. Heppeler, J.S. Schmitt, H.R. Mäcke, Affinity profiles for human somatostatin receptor subtypes SST1–SST5 of somatostatin radiotracers selected for scintigraphic and radiotherapeutic use, Eur. J. Nucl. Med. 27 (3) (2000) 273–282.
[9] V. Kubíček, J. Havlíčková, J. Kotek, G. Tircsó, P. Hermann, É. Tóth, I. Lukeš, Gallium (III) complexes of DOTA and DOTA– monoamide: kinetic and thermodynamic studies, Inorg. Chem. 49 (23) (2010) 10960–10969.
[10] S. Niedermoser, J. Chin, C. Wängler, A. Kostikov, V. Bernard-Gauthier, N. Vogler, J.-P. Soucy, A.J. McEwan, R. Schirrmacher, B. Wängler, In vivo evaluation of 18F-SiFAlin–modified TATE: a potential challenge for 68Ga-DOTATATE, the clinical gold standard for somatostatin receptor imaging with PET, J. Nucl. Med. 56 (7) (2015) 1100–1105.
[11] D. Andreu F. Albericio N.A. Solé M.C. Munson M. Ferrer G. Barany Formation of disulfide bonds in synthetic peptides and proteins M.W. Pennington B.M. Dunn Peptide Synthesis Protocols 35 Humana Press New Jersey 91 170.